Chinese Chemical Letters 33 (2022) 3031–3034

Contents lists available at ScienceDirect

Chinese Chemical Letters

journal homepage: www.elsevier.com/locate/cclet

A novel strategy for high-specificity, high-sensitivity, and high-throughput study for gut microbiome metabolism of aromatic carboxylic acids

Ningning Zhao[a,b], Zhiqiang Liu[a,b,c], Junpeng Xing[a], Zhong Zheng[a], Fengrui Song[a], Shu Liu[a,*]

[a] National Center of Mass Spectrometry in Changchun and Jilin Provincial Key Laboratory of Chinese Medicine Chemistry and Mass Spectrometry, Changchun Institute of Applied Chemistry, Chinese Academy of Sciences, Changchun 130022, China
[b] Institute of Applied Chemistry and Engineering, University of Science and Technology of China, Hefei 230029, China
[c] State Key Laboratory of Electroanalytical Chemistry, Changchun Institute of Applied Chemistry, Chinese Academy of Sciences, Changchun 130022, China

ARTICLE INFO

Article history:
Received 16 April 2021
Revised 10 August 2021
Accepted 6 September 2021
Available online 10 September 2021

Keywords:
Aromatic carboxylic acids
Gut microbiome
Dual-template and double-shelled molecularly imprinted 96-well microplate
Stable isotope labeling derivatization
UHPLC-TQ MS

ABSTRACT

Aromatic carboxylic acids (ACAs) may be as transformed key metabolites *via* gut microbiome for playing better pharmacological effects. However, it's rare to achieve high-specificity, high-sensitivity, and high-throughput detection simultaneously, especially, for tracing trace ACAs in gut microbiome. In this work, firstly, a novel dual-template and double-shelled molecularly imprinted 96-well microplates (DDMIPs) was designed and amplified signal for *p*-hydroxybenzoic acid (PBA) and 3,4,5-trimethoxycinnamic acid (TMA). Additionally, the DDMIPs and a stable isotope labeling derivatization (SILD) method combined with the ultra-high performance liquid chromatography triple quadrupole tandem mass spectrometry (UHPLC-TQ MS) was firstly stepwise integrated, achieving high-effective, high-sensitive, and high-throughput study of gut microbiome metabolism. The whole strategy showed lower limits of detections (LODs) up to 1000 folds than the traditional method, and revealed a more real metabolism-time profile of PBA and TMA by 3-step signal amplification. The platform also laid the foundation for fast, simple, high-selective, high-effective, and high-throughput metabolism and pharmacological research.

Gut microbiota, as "second brain", plays a crucial role in the regulation of central nervous system (CNS), especially for depressive disorder, and psychiatric disorders [1-3]. It also plays an important role in the metabolism of oral prodrugs. However, most natural oral prodrugs are difficult to be absorbed and detected *in vivo* [4]. Accordingly, the pharmacodynamic mechanism of some prodrugs is not clear or not exact, who plays the ultimate role. Nowadays, some aromatic carboxylic acids (ACAs) have gradually been studied, as key gut microbiota metabolites, by incubating some herbs with/without gut microbiome [5-10]. However, low oral utilization of most drugs, the complex matrix effect, the high-abundance interfering compounds, trace metabolites ACAs, and large-scale samples from time series of incubation limit their real-time monitoring and analysis. Therefore, it would be a promising exposure to develop a high-selective, high-efficient, and high-throughput method for the study of key metabolite ACAs *via* gut microbiome.

Recently, surface molecularly imprinted polymers (SMIPs) have been widely used in separation, because of their outstanding performance including more accessible sites, specific cavities, high stability, fast mass transfer, and good reproducibility [11–17]. Due to the imprinting ability is still not up to the analysis of some trace molecules, the dual-template spherical or double-shelled SMIPs are few designed by meaningful template molecules and ethylene imine polymer (PEI), polydopamine (PDA), and hydrophilic resins forming layer of molecularly imprinted polymers (MIPs) [18–20]. Additionally, although the spherical MIPs have been further applied to separate targets, the reproducibility is limited by the continuous elution. The SMIPs based on the 96-well microplates came into being, and have been designed and applied for the high-throughput enrichment of melamine, enzyme-linked immunosorbent assay, respectively [21–23]. But they are rarely enriched other substances, especially for ACAs. Thus, it is desirable for high-throughput adsorption of ACAs by 96-well molecularly imprinted microplates. However, due to the nature of ACAs, few reports designed SMIPs

* Corresponding author.
E-mail addresses: mslab20@ciac.ac.cn, 1985liushu@163.com (S. Liu).

https://doi.org/10.1016/j.cclet.2021.09.022
1001-8417/

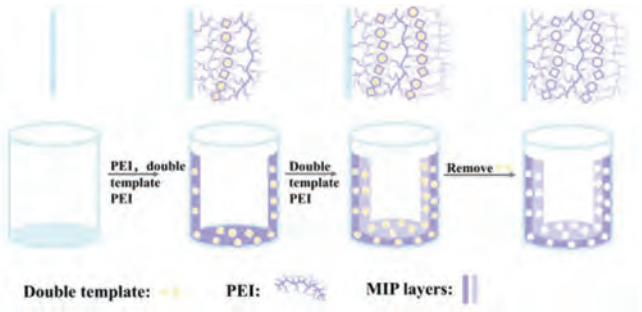

Fig. 1. The synthetic route for DDMIPs.

for highly sensitive analysis of ACAs, and even it's rarely for high-throughput enrichment of trace metabolites ACAs in bio-samples [24–26].

To date, the reported quantitative research for normal content of ACAs was implemented through high-performance liquid chromatography-diode array detection (HPLC-DAD) method [27,28], but quantitative analysis for trace ACAs was implemented through HPLC-triple quadrupole tandem mass spectrometry (HPLC-TQ MS) technology in negative ion mode combined with/without solid-phase extraction (SPE) method [29,30]. The high-sensitive analytical technology combined with the novel separation method has improved accuracy and sensitivity for trace ACAs in bio-samples. It has overcome some of the issues mentioned earlier. However, the improved sensitivity of detection for targets cannot meet our quantitative requirements for targets with lower content, and it still faces problems, which the polarity of ACAs is greater, and causes overlap of chromatographic peaks for a short time, even some peaks are not retained on the chromatogram. Some papers have reported chemical derivatization methods for fatty acids [31–34]. Our group previously proposed stable isotope labeling derivatization (SILD) method combined with ultra-HPLC-MS/MS (UHPLC-TQ MS) method have been proved to provide higher accuracy and sensitivity for greatly improving pharmacodynamic understand of ACAs under mild conditions [35]. It employed deuterated derivatization products as the internal standard (ILIS) of targets, eliminated endogenous ACAs in blank bacteria, and avoided the error by the endogenous ACAs itself as the internal standard. Therefore, the SILD combined with UHPLC-TQ MS method may be a potential value for further increased sensitivity for ACAs in bio-samples.

In this study, a novel quantitative strategy for *p*-hydroxybenzoic acid (PBA) and 3,4,5-trimethoxycinnamic acid (TMA) was designed for highly effective, highly sensitive and high-throughput study of tenuifoliside A (TA) incubated with gut microbiome. Firstly, a novel dual-template (PBA and TMA) and double-shelled molecularly imprinted 96-well microplates (DDMIPs) were designed and synthesized. Integrating the dual-template, the multivalent cavities-based PEI dendrimer, double-shelled layers, and multi-parallel wells, it amplified signal on the high-throughput platform for PBA and TMA. Secondly, the SILD was further increased sensitivity. And it adopted the isotope-labeled standards as internal standards, making the results more accurate. Finally, the UHPLC-TQ MS was used to improve again the accuracy of analytical data to reveal a real metabolism-time profile of metabolites PBA and TMA.

The synthetic route for DDMIPs was shown in Fig. 1. The first layer PEI was used both as the first imprinting layer and as the functional monomer of DDMIPs. The dual-template and double-shelled surface molecularly non-imprinted polymers on 96-well microplates (DDNIPs), the dual-template and single-shelled SMIPs on 96-well microplates (DSMIPs), and the dual-template and single-shelled surface molecularly non-imprinted polymers on 96-well microplates (DSNIPs) were also prepared. The polystyrene (PS) based 96-well microplates and prepared DDMIPs can be clearly seen in Figs. S1 and S2A (Supporting information). Because their characteristics were almost the same, so we did not give the data of DDNIPs. Apart from PS based 96-well microplate, the DDMIPs and DSMIPs are rough, and the degree of density is obviously different (DDMIPs > DSMIPs), reflecting that the double-shelled SMIPs is relatively more uniform than single-shelled SMIPs. Meanwhile, the energy dispersive X-Ray spectroscopy (EDS) image and qualitative data of element composition (Figs. S2B and C in Supporting information), reflected that relative standard deviations (RSDs) for percentage content of C, N, O and Si, were $\leq$ 9.21% and 12.37% in different wells of one DDMIPs, and in wells of different batches DDMIPs microplates, respectively. The typical Fourier-transform infrared (FT-IR) peak of Si-O-Si, N–H bond was obviously observed at ~1130 cm^{-1}, 3100–3600 cm^{-1}, respectively. What is more, the typical peaks of C 1s (~284 eV), N 1s (~400 eV), O 1s (~532 eV), and Si 2p (~102 eV) were also obviously observed in X-ray photoelectron spectroscopy (XPS) spectrum, which proved once again that DDMIPs were successfully synthesized (Fig. S3 in Supporting information).

In Tables S1 and S2 and Figs. S4–S6 (Supporting information), the primary experiments were estimated, including the conditions of UHPLC-TQ MS, calibration curves, effect of different 96-well microplates on adsorption capacities, and optimization of the synthesis conditions. Finally, the best imprinting capacities of DDMIPs were confirmed. And 1% (the content of first layer), 0.5% (the content of second layer), 3 h (the polymerization time of first layer) and 4 h (the polymerization time of second layer) were selected to synthesize DDMIPs for further research.

As shown in Fig. 2, the isothermal equilibrium experiments and adsorption kinetic experiments were performed. When the concentration was more than 1.32 μmol/L, and 0.74 μmol/L, the equilibrium adsorption capacity (Q_e) was continuously decreased for DDMIPs. Meanwhile, when the concentration of PBA and TMA was more than 0.61 μmol/L and 0.31 μmol/L, the Q_e was also continuously decreased for DDNIPs. It is demonstrated that the imprinting balance was reached at this concentration, respectively. With imprinting time was continuously increasing, the Q_e of DDMIPs and DDNIPs was gradually attended to saturation at 30 min for PBA and TMA. What is more, the Q_e of DDMIPs (88%) was more than the Q_e of DDNIPs (49.3%) for PBA, and the Q_e of DDMIPs (40.6%) was also more than that of DDNIPs (20.7%) for TMA, respectively.

The imprinting rate was faster from 0 min to 10 min than the rate during 15 min to 30 min for PBA and TMA. And the imprinting rate was faster for DDMIPs than that of DDNIPs. All the results suggested that there were more capacities in double-shelled SMIPs rather than in single-shelled SMIPs microplates, and the second layer did not bury the cavities of the first layer. Subsequently, the elution time was also investigated for DDMIPs and DDNIPs. As shown in Fig. S7 (Supporting information), 30 min exhibited the best elution effect for PBA and TMA. So, both imprinting time and elution time were set at 30 min.

As shown in Fig. S8A (Supporting information), imprinting selectivity of DDMIPs and DDNIPs for PBA and TMA were assessed by structural analogs (ferulic acid (FA), cinnamic acid (CA), sinapic acid (SA), benzoic acid (BA), 4-methoxycinnamic acid (PMA) and *p*-coumaric acid (PCA)). Chemical structures of PEI and ACAs are shown in Fig. S9 (Supporting information). The Q_e of PBA and TMA onto DDMIPs (1 μmol/L and 0.52 μmol/L) was the highest than Q_e of other adsorbates. It's also higher than Q_e of PBA and TMA onto DDNIPs (0.46 μmol/L and 0.24 μmol/L). It is confirmed that the DDMIPs have specific imprinting ability for PBA and TMA. Furthermore, the specific imprinting performance was also estimated by Qe, the imprinting factor (IF) and the selectivity coefficient (SC) in Table S3 (Supporting information). DDMIPs and DDNIPs both have the highest imprinting capacities for templates than others. The

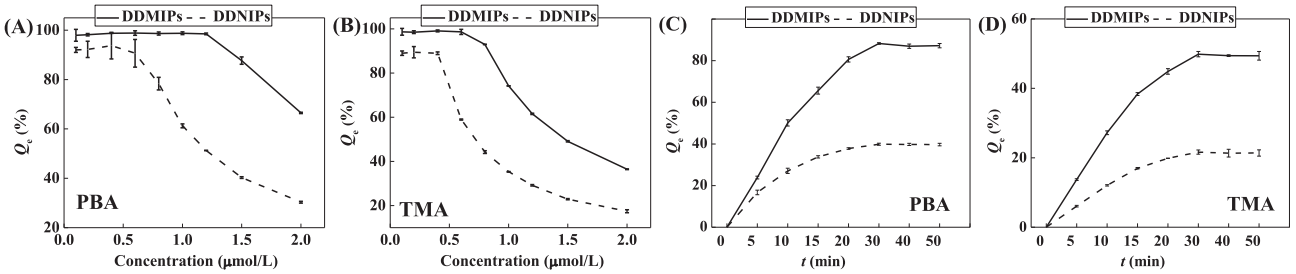

Fig. 2. Isothermal curves for binding PBA and TMA onto DDNIPs and DDMIPs (A, B). Adsorption kinetic curves for binding PBA and TMA onto DDNIPs and DDMIPs (C, D).

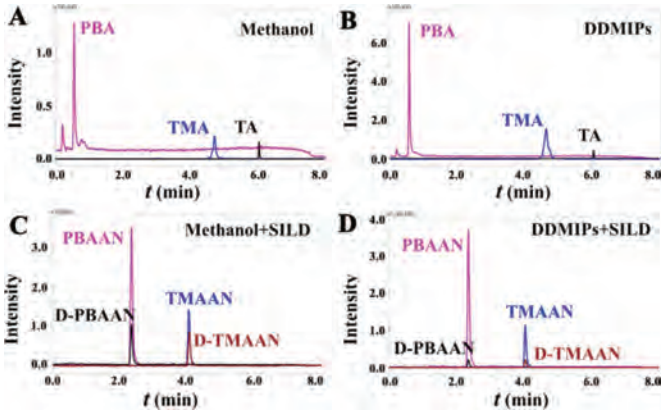

Fig. 3. MRM chromatograms for real gut microbiome samples by methanol, DDMIPs, methanol combined with SILD, and DDMIPs combined with SILD strategies.

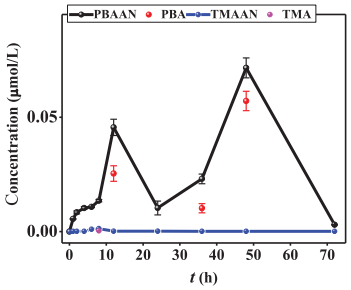

Fig. 4. The metabolic profiles of PBA and TMA before and after processing with this DDMIPs and SILD combined with UHPLC-TQ MS technology.

IF values of PBA and TMA were 2.20 and 2.18, and the SC values were 0.99 and 1.01, respectively. Although all the ACAs could be adsorbed (attributed to a partial structure similar to that of PBA or TMA), the DDMIPs have the highest imprinting selectivity for PBA and TMA.

In Table S4 and Figs. S8B and C (Supporting information), the reproducibility, regeneration and reusability performance were further evaluated for DDMIPs and DDNIPs. It is kind of like a kit, unlike particles, which require additional operating steps and cost. Hence, the reproducibility, regeneration and reusability performance were satisfactory with interaction, suitable cavities, and imprinted processes.

Based on the previous report [35], and the specific imprinting experiment by DDMIPs, the peak shape of ACAs is not good. The DDMIPs and the SILD method combined with UHPLC-TQ MS were integrated to obtain a good chromatogram for further precise and sensitive quantification with deuterated derivatives as corresponding ACAs internal standard. As shown in Tables S5–S8 and Figs. S10 and S11 (Supporting information), by directly imprinting targets without protein deposition, concentration, and re-dissolution, the methodological verification was successful, revealing that the novel strategy was very likely to have a qualitative breakthrough in the quantification of ACAs.

Additionally, the practicability of different methods was further evaluated by dealing with real gut microbiome samples by methanol, DDMIPs, methanol combined with SILD, and DDMIPs combined with SILD strategies. As shown in Fig. 3 and Table S9 (Supporting information), the content of DDMIPs was higher than that of methanol method for PBA and TMA, respectively (Figs. 3A and B). It is desirable for the first signal amplification by the DDMIPs strategy mainly due to the following three advantages: (1) MIPs in wells can nearly completely remove the template, and produce the specifically recognizable and memorable three-dimensional (3D) cavities; (2) they possess high affinity, selectivity, stability, and reusability for PBA and TMA; (3) multiple-well microplates provide a high-throughput capability for analysis of large-scale samples, saving reagents, labor, and time. As shown in Figs. 3C and D and Table S9, the content of novel strategy was higher than that of methanol combined with SILD method for PBA and TMA, respectively. Besides, the content of the novel strategy was higher than that of DDMIPs method. The results demonstrated that SILD method not only improved the chromatographic behavior of the targets, but further increased sensitivity. Especially, the advanced analytical technology (UHPLC-TQ MS) was used to improve again quantitative sensitivity. From this, the integrated strategy is able to achieve 3-step amplification of the signal as expected.

After successful validation, the DDMIPs in 96-well microplates and SILD combined with the UHPLC-TQ MS technology were applied to study the metabolic profiles of PBA and TMA in Fig. 4. By the novel strategy, the derivative of PBA (PBAAN) and derivative of TMA (TMAAN) could be monitored and determined during 0–72 h, and excluded the interference of blank samples. On the contrary, the monitoring for PBA and TMA was not accurate by normal method, because ACAs could only be detected at the highest concentration points above their limit of detection. It suggested that our novel strategy was feasible for gut microbiome research, especially for trace targets. It successfully achieved 3-step signal amplification, as follows: At the first signal amplification, the DDMIPs could delt with all the samples at 13 time points ($n = 6$), simultaneously. And, it could provide enough cavities based double-shelled PEI layers and 96 well, for PBA and TMA to specific imprinting targets. At the second increased sensitivity, the SILD method made targets be derivatized to accurately quantify by ILIS, and eliminated the interference of ACAs in blank samples. In the third step, the UHPLC-TQ MS improved sensitivity for PBA and TMA again.

As shown in Fig. 4, the concentration of PBAAN was far above that of TMAAN. From the change of content, it's inferred that PBA may play a more important role than TMA in regulation *via* gut microbiome *in vivo*. It is needed further verification in terms of biology. By the novel strategy, two peaks of PBAAN and TMAAN re-

vealed a real pharmacological process in comparison with the normal method. At the high point, it may be attributed to synthesis of ester bonds more than hydrolysis or other activities of ACAs. The real-time monitoring for metabolic products ACAs accurately revealed the real pharmacodynamic mechanism of TA by our strategy.

The advantages and disadvantages for normal methanol, magnetic MIPs, SILD and our novel strategies were shown in Table S10 (Supporting information). The analytical technologies are constantly being improved, from single-by-single methanol method (fussy procedures) to magnetic MIPs, and the method based 96-well microplates without protein precipitation from centrifugal separation with expensive equipment to fast magnetic, or direct-suction separation technique, from direct quantification to more accurately quantification, from random enrichment to specific imprinting by a large number of fixed cavities, and so on. Importantly, it exhibited lower limits of detections (LODs) up to 1000 folds, and more accurately quantitative results for real bio-samples than previous methods.

In this work, the DDMIPs were firstly designed and synthesized. Additionally, it and SILD with the advanced UHPLC-TQ MS technology were successfully applied for study of a large-scale of gut microbiome samples. The novel strategy amplified 3-step signal to specific, high-throughput, and accurate monitor derivatized targets. The sensitivity was improved up to 1000 folds than the traditional method. And more, from the change of chemical composition, the real metabolic mechanism of TA *via* gut microbiome was inferred that the transformed PBA and TMA might be active metabolites. It laid the foundation for further pharmacological research. Importantly, this study opens up a new mode for fast, high-specific, high-sensitive, high-throughput, and targeted-derivatization for 3-step signal amplification of trace ACAs from bio-samples. It also provides a valuable strategy for more actual quality control and research on pharmacology and mechanism.

Declaration of competing interest

The authors declare that they have no known competing financial interests or personal relationships that could have appeared to influence the work reported in this paper.

Acknowledgments

This work was supported by grants from the National Natural Science Foundation of China (Nos. 82073973, 81872969), and the Jilin Provincial Industrial Innovation Special Fund Project (No. 20200703015ZP) and the Science and the Youth Innovation Promotion Association of CAS (No. 2019227).

Supplementary materials

Supplementary material associated with this article can be found, in the online version, at doi:10.1016/j.cclet.2021.09.022.

References

[1] V. Ridaura, Y. Belkaid, Cell 161 (2015) 193–194.
[2] Z. Yang, J. Li, X. Gui, et al., Mol. Psychiatry 25 (2020) 2759–2772.
[3] L. Pan, P. Han, S. Ma, et al., Acta Pharm. Sin. B 10 (2020) 249–261.
[4] Z.X. Zhao, J. Fu, S.R. Ma, et al., Theranostics 8 (2018) 5945–5959.
[5] J.B. Yu, Z.X. Zhao, R. Peng, et al., Front. Pharmacol. 10 (2019) 268.
[6] Q. Cui, Y. Pan, X. Xu, et al., Fitoterapia 109 (2016) 67–74.
[7] Y. Li, G. Zhou, S. Xing, P. Tu, X. Li, J. Agric. Food Chem. 63 (2015) 6764–6771.
[8] X. Wang, X. Chang, X. Luo, et al., Front. Pharmacol. 10 (2019) 826.
[9] S. Chandra, A. Roy, M. Jana, K. Pahan, Neurobiol. Dis. 124 (2019) 379–395.
[10] E. Mhillaj, S. Catino, F.M. Miceli, et al., Mol. Neurobiol. 55 (2018) 905–916.
[11] M. Zhao, S. Huang, H. Xie, et al., Anal. Chem. 92 (2020) 10540–10547.
[12] K.Z. Chin, S.M. Chang, ACS Appl. Nano Mater. 2 (2019) 89–99.
[13] Q. Huang, Z. Zhao, D. Nie, et al., Anal. Chem. 91 (2019) 4116–4123.
[14] M. Liu, S.B. Torsetnes, C. Wierzbicka, et al., Anal. Chem. 91 (2019) 10188–10196.
[15] V. Pichon, N. Delaunay, A. Combes, Anal. Chem. 92 (2020) 16–33.
[16] J.J. BelBruno, Chem. Rev. 119 (2019) 94–119.
[17] Y. Zhang, D. Liu, J. Peng, et al., Talanta 209 (2020) 120555.
[18] L. Guo, X. Ma, X. Xie, et al., Chem. Eng. J. 361 (2019) 245–255.
[19] H.Y. Wang, P.P. Cao, Z.Y. He, et al., Nanoscale 11 (2019) 17018–17030.
[20] C. Jia, M. Zhang, Y. Zhang, et al., ACS Appl. Mater. Interfaces 11 (2019) 32431–32440.
[21] X. Bi, Z. Liu, Anal. Chem. 86 (2014) 12382–12389.
[22] X. Bi, Z. Liu, Anal. Chem. 86 (2014) 959–966.
[23] J. Yu, C. Zhang, P. Dai, S. Ge, Anal. Chim. Acta 651 (2009) 209–214.
[24] Y.Z. Zhang, B. Qin, B. Zhang, et al., Anal. Chim. Acta 1096 (2020) 193–202.
[25] X. Liu, F. Wu, C. Au, et al., J. Appl. Polym. Sci. 136 (2019) 46984.
[26] H. Li, R. Long, C. Tong, et al., Talanta 194 (2019) 969–976.
[27] J.B. Weon, H. Park, H.J. Yang, J.Y. Ma, C.J. Ma, J. Nat. Med. 65 (2011) 375–380.
[28] J.B. Weon, H.J. Yang, J.Y. Ma, C.J. Ma, J. Nat. Med. 66 (2012) 510–515.
[29] J. Guan, L. Wang, J. Jin, et al., J. Pharm. Biomed. Anal. 170 (2019) 1–7.
[30] E. Lamy, L. Pilyser, C. Paquet, E. Bouaziz-Amar, S. Grassin-Delyle, Talanta 224 (2020) 121881.
[31] S. Zhu, Z. Zheng, H. Peng, et al., J. Chromatogr. A 1616 (2020) 460794.
[32] J. Leng, H. Wang, L. Zhang, et al., Anal. Chim. Acta 758 (2013) 114–121.
[33] Y. Xu, L. Sun, X. Wang, et al., Talanta 199 (2019) 97–106.
[34] Q.F. Zhu, Z. Zhang, P. Liu, et al., J. Chromatogr. A 1460 (2016) 100–109.
[35] N. Zhao, T. Zhao, M. Fan, et al., Talanta 224 (2020) 121791.